

**" Sixth Workshop on Non-Linear Dynamics and
Earthquake Prediction"**

15 - 27 October 2001

**Simplicity Out of Complexity:
The Example of Geomagnetic Series**

J.-L. Le Mouél

**Institut de Physique du Globe
Paris, France**

The irregular variations of the external geomagnetic field from Intermagnet data

E. Bellanger, F. Anad, J.-L. Le Mouél, M. Manda

Institut de Physique du Globe de Paris, France.

Abstract. The INTERMAGNET program publishes each year a CD-ROM containing homogeneous series from a number of magnetic observatories (76 in 1999). These series are definitive minute values of the three components of the geomagnetic field. We transform these series using a simple nonlinear analysis tool [Blanter *et al.*, submitted] and obtain, as in a former study of daily averages [Bellanger *et al.*, 2001], a remarkable simple activity field $\Omega(P, t)$ whose space and time variables separate. We briefly discuss the space and time properties of this field.

1. Introduction

In a former paper [Bellanger *et al.*, 2001], we constructed homogeneous series from the daily averages of the three components of the magnetic field at a number of observatories P , processed them with a simple nonlinear tool, and finally obtained a field $\Omega(P, t)$ which we called an activity field. $\Omega(P, t)$ appeared to be the product of a time function $R(t)$ by a space function $\omega(P)$ with quite simple a geometry.

The INTERMAGNET program publishes each year a CD-ROM containing the minute values of the components of the magnetic field recorded in some 80 observatories. Starting from these minute values we apply the same lines of reasoning as in Bellanger *et al.* [2001], to see whether a simple structure, in space and time, can be simply extracted from this big body of data, as it was the case using daily values.

2. The data

All modern magnetic observatories use similar instrumentation to produce similar data products. The recorded fundamental measurements are one-minute values of the vector components and of the scalar intensity of the field. The one-minute data are important for studying variations of the external geomagnetic field, such as the daily variation and the magnetic storms. From the one-minute data, hourly, daily, monthly and annual mean values are produced. It is the monthly and annual mean values which capture the secular variation

of the main field emanating from the Earth's core.

The INTERMAGNET program calls for the world's magnetic observatories to be equipped with fluxgate and proton magnetometers (with a resolution of 0.1 nT) operating automatically under computer control. To prevent aliasing of the minute values a numerical filter is required; a minute value is obtained by applying a Gaussian filter of 19 coefficients to a series of 19 measurements sampled every 5 seconds and centered on the given minute. Minute values are given in tenths of nT. Data should be available locally for quality control and local use, but should also be transmitted to a regional Geomagnetic Information Node (GIN) where they are collected.

The number of observatories participating in this program has continuously increased, from 41 in 1991 to 76 in 1999. The INTERMAGNET CD-ROM only contains data from participating observatories. These data are definitive one-minute values (data which have been corrected for baseline variations and which have had spikes removed and gaps filled where possible), with an absolute accuracy of ± 5 nT, of the three field components: horizontal northward (X), horizontal eastward (Y) and vertical downward (Z). For a full description see the INTERMAGNET Technical Manual [Trigg and Coles, 1999] and the INTERMAGNET web site (<http://www.intermagnet.org>). For observatory practice, see Jankowski and Sucksdorff [1996].

In the present study we use a set of 30 INTERMAGNET observatories providing a reasonably homogeneous distribution at the Earth's surface, for the 1996-1997

time-span. The distribution of the observatories, with their IAGA code is given in figure 10. Moreover a six-year series for Chambon la Forêt observatory has been analysed.

3. The absolute derivative

We have $3 \times M$ series $X_m(t_n)$, $Y_m(t_n)$, $Z_m(t_n)$, $m = 1, 2 \dots M$; M is the number of observatories; t_n is time, reckoned in minutes; the range of n is different for each observatory. Let $F(t)$ be one of these time-series and consider the first difference $F'(t)$ (we will call $F'(t)$ derivative; but we do not look for a better estimate of the time derivative, by using for example classical several points formulae; in fact, we are considering ranges), the absolute first difference $|F'(t)|$:

$$F'(t) = F(t+1) - F(t), \quad (1)$$

$$|F'(t)| = |F(t+1) - F(t)|, \quad (2)$$

and the average of $|F'(t)|$ in a sliding time window of length T [Blanter *et al.*, submitted],

$$|F'(t)|_T = \frac{1}{T} \sum_{\tau=0}^{T-1} |F'(t+\tau)|. \quad (3)$$

$|F'(t)|_T$ is defined at $(N-T)$ points (N is the length of the time-series). In the present study, T is taken equal to 1 day, *i.e.* $T = 1440$.

4. Results

Some of the results are illustrated by figures 1 and 2. The graphs represent $|X'|_T$, $|Y'|_T$, $|Z'|_T$ as computed by (3), t being reckoned in minutes, in different observatories.

It is remarkable how the $|X'|_T$, $|Y'|_T$, $|Z'|_T$ curves look alike in a given observatory, but also how all the curves, for all the observatories, look alike, even in tiny details. Figure 3 gives an enlarged representation of three $|X'|_T$ curves relative to Chambon la Forêt (CLF), Kakioka (KAK) and Sodankylä (SOD), located respectively in France, Japan and Finland. The fact that the averaging over T is what draws the simple global structure of the series is made clear by figures 4 and 5. Figure 4 represents $X'(t) \equiv X(t+1) - X(t)$, $|X'(t)| = |X(t+1) - X(t)|$, $Y'(t)$ and $|Y'(t)|$ in CLF for the first fortnight of year 1996. Only a family air exists between the graphs of $X'(t)$ and $Y'(t)$. Figure 5 represents three "phase diagrams" ($X'(t)$, $Y'(t)$), ($|X'(t)|$, $|Y'(t)|$) and ($|X'|_T$, $|Y'|_T$) for two disturbed days in CLF. No polarisation can be derived from the two first diagrams,

whereas a clear linear polarisation appears when a 1-day averaging of the absolute derivatives is performed. The linear polarisation is conserved, when considering two years of data (1996–1997) and the correlation coefficients between different components in a given observatory are better than 0.90 (figure 6).

In order to get an estimate of the correlation between series from different observatories, we draw polarisation diagrams and compute the corresponding cross-correlation values. Considering for example $|X'|_T$ in CLF and $|X'|_T$ in KAK (illustrated by figure 7), the correlation coefficient is 0.93. Let us stress that, although the curves are alike, and that almost all features can be recognized from a curve to another, they are not identical; we are looking at real data.

A strong advantage of considering the absolute derivative (or first difference) from one-minute values is that it practically does not rely on the absolute values of the magnetic measurements, *i.e.* on good baselines. A slow drift of these baselines will have a small but negligible effect on $|F'(t)|$ and $|F'(t)|_T$. As for the short-term behaviour of baselines, it is rather easy to control it; furthermore, the baselines have been carefully examined when submitted to the INTERMAGNET CD-ROM committee.

5. The reference level and UT dependence

To be simple, let us just recall that transient variations of the external geomagnetic field can be classified as regular and irregular variations [Mayaud, 1978]; the former are due to permanent sources of field which cause the regular occurrence, every day, of a certain variation during certain local times at a given point on the Earth; the latter are generated by sources which do not permanently exist, and, hence, their occurrence is basically irregular.

Let us write,

$$\mathbf{B}_e(\mathbf{r}, t) = \mathbf{S}_R(\mathbf{r}, t) + \mathbf{D}(\mathbf{r}, t), \quad (4)$$

\mathbf{r} is the position vector, t is time, \mathbf{B}_e is for the external field, \mathbf{S}_R for the regular field, \mathbf{D} for the irregular (disturbance) one. We will briefly come back to the content of \mathbf{D} in section 7. A drawback of using an absolute derivative as (2) or (3) is that, the additivity property being lost, it is not so easy to separate the contributions of the two components of (4). Let us look at some orders of magnitude. \mathbf{S}_R is supposed regular; let us consider that it cannot give raise to variations of 50 nT in less than 3 hours. Its contribution to $|F'(t)|$ is then

smaller than 0.28 nT/min. As for the measurement error, it comes from section 2 that its contribution to the differences $|F(t+1) - F(t)|$ and $|F'(t)|_T$ can be estimated to 0.14 nT/min. It can then be supposed that the value of $|F'(t)|_T$, in the case of a null \mathbf{D} field (over a day) is of the order of 0.3 nT/min. Looking at the graphs of figure 1 and 2, it appears that in most stations the reference level (defined as the lower envelope of the curves) has an ordinate of this order of magnitude (in fact, in most cases, lesser).

In the following, we consider that the departures of the curves from the so defined reference level are representative of the \mathbf{D} field. We check that these variations are mostly in universal time. Figure 8 represents the correlation coefficient $c(\theta)$ between $|X'(t)|_T$ in Chambon la Forêt and $|X'(t+\theta)|_T$ in Kakioka, in function of θ for a period of 15 perturbed days (in UT). It appears that $c(\theta)$ is maximum for time shifts close to 1 hour, whereas the longitude difference between Chambon la Forêt and Kakioka is close to 9 hours. We might attribute this shift of 1 hour to a remaining contamination by the \mathbf{S}_R .

6. The field $\Omega(P, t)$

Let us denote $\Omega(P, t)$ the field of the $(|X'|_T(P, t); |Y'|_T(P, t); |Z'|_T(P, t))$, where P is the position. It is derived from \mathbf{D} as stated above. Since at each observatory, for each component (in a first but good approximation), the temporal variations are similar, it follows that, at the same approximation, the time and space variations of $\Omega(P, t)$ separate:

$$\Omega(P, t) = \omega(P)R(t). \quad (5)$$

$R(t)$ is taken positive (an activity function), $\omega(P)$ characterizes the geometry of the irregular variations processed as indicated.

6.1. Geometry

In *Bellanger et al.* [2001], we made a (rather qualitative) analysis of the field $\omega(P)$ in the case of daily means, and showed that it presented an axial symmetry around an axis whose colatitude and longitude were $(14 \pm 3; -82 \pm 10)$ degrees. Things appear less simple here. It should be said that $\Omega(P, t)$ is a rather special field (an activity field, as already said, which cannot be analysed as straightforwardly as classical fields). We just present here a first step to the analysis of $\omega(P)$.

At each point P we compute the direction of $\omega(P)$ in the following way: we determine the declination D (and in a similar way the inclination I) of ω by computing the

regression line of the graphs representing $|Y'|_T$ versus $|X'|_T$ (figure 6); denoting $(|Y'|_T/|X'|_T)_{\text{ex}}$ the slope of the regression line, D is taken as

$$D = \tan^{-1} ((|Y'|_T/|X'|_T)_{\text{ex}}). \quad (6)$$

Six examples of regression computation are presented on figure 6. The error on the estimation of the slopes is small enough for the precision being better than 3 degrees in D and I . These estimates are free from the value of the reference level as defined in 5, *i.e.* of the intercepts of the regression lines with the x and y axes.

We also estimate the length of the horizontal component of ω , $\|\omega_{\perp}\|$, in the following way,

$$\|\omega_{\perp}\| = \sqrt{|X'|_T^2 + |Y'|_T^2}, \quad (7)$$

introducing a bias due to the reference level. It is to be noted that all the quantities $|X'|_T(t)$, $|Y'|_T(t)$ and $|Z'|_T(t)$ are positive by construction. The cartesian components of ω are defined only within a multiplicative factor ± 1 . There are four possible values for D and two for I (figure 9). In fact, the number of combinations is reduced from eight to four, since there is no need to distinguish between ω and $-\omega$. In *Bellanger et al.* [2001] we used simple regularity conditions to discriminate between the four possible situations at each observatory. It is less simple here. We just present, on the map of figure 10, a chosen direction and the length of the horizontal component ω_{\perp} of ω , taking systematically both X and Y , the components of ω_{\perp} , positive. (symmetric orientations with respect to Ox or Oy axes are possible when analysing an individual station). We will come back to this problem later, after gathering all the available data series; methods like the ones developed in *Hulot et al.* [1997] and *Khokhlov et al.* [1997] could be used.

A conspicuous feature of the map is the large intensity of ω_{\perp} in high latitudes (auroral regions). Nevertheless, the curves of high latitudes look alike the other ones (see *e.g.* figure 3 where $|X'|_T$ in Sodankylä, Finland, colatitude 22.63 degrees, can be compared to $|X'|_T$ in mid-latitudes observatories: Chambon la Forêt, colatitude 41.98 degrees and Kakioka, colatitude 53.77 degrees) — see section 7.

6.2. Recurrences

Let us briefly elaborate on the temporal behaviour of our activity field, *i.e.* function $R(t)$ of (5). Some kind of average of a number of $|X'|_T$, $|Y'|_T$, $|Z'|_T$ curves could be taken; we will simply take as representative the curve $|Y'|_T$ in Chambon la Forêt.

We consider the 6-year long series of the $|Y(t+1) - Y(t)| = |Y'(t)|$, without averaging over a day. Figure 11 represents the spectrum of $|Y'(t)|$. Expected peaks can be recovered at 1 day (and harmonics), 27 days (and harmonics), and probably one year and six months, although the length of the series, 6 years, is rather short for revealing such long periods with a simple Fourier transform. These periodicities are well known and we won't discuss them in any details in this paper devoted to short time constant (events of duration less than a few days, see figures 1 and 2) variations of the irregular field. Nevertheless, our array of INTERMAGNET observatories will allow us to study in a new way the geographical distribution of the intensity of these spectral peaks [Banks, 1969; Achache et al., 1981; Olsen, 1999].

7. Discussion and perspectives

We will not try to give a full interpretation of our main results, which are the strong resemblance of all the $|X'|_T, |Y'|_T, |Z'|_T$ curves, and the smooth variation of the $\omega_{\perp}(P)$ field (despite the ambiguity in the direction of this vector, we can say that it is locally smooth), but make only a few comments and point out some perspectives.

At the end of section 6.1, we emphasized the strong values of $\omega_{\perp}(P)$ in the high latitude observatories. Following Fukushima and Kamide [1973], let us write the world geomagnetic disturbance field D as:

$$D = D_R + D_P + (D_{CF} + D_T), \quad (8)$$

D_R is the geomagnetic disturbance field generated by a ring current flowing in the geomagnetic equatorial plane at a geocentric distance of several Earth's radii. D_P is the geomagnetic disturbance caused primarily by intense electrojets flowing in the ionosphere of the polar region (including the auroral zone) and their accompanying currents in the ionosphere or magnetosphere, or both. D_{CF} and D_T fields can generally be neglected at the Earth's surface.

Our observations show that D_P plays an important part in our $\Omega(P, t)$ field (high values in high latitudes), and that D_R and D_P are intimately correlated (high resemblance between curves from all latitudes), which is maybe to be expected if the corresponding current systems are physically linked.

Let us have a look at conservation properties. It does not make sense to look at conservation properties of $|Y'(t)|_T$ with a minute sampling and an averaging over 1 day. Let us rather consider the series of daily

values

$$Y^*(k) = |Y'(o(k))|_T \quad (9)$$

time $o(k)$ being 0h00:01 of day k . It is clear, from the way it is computed, that $Y^*(k)$ is a good estimate of the activity range of Y for day k (in fact, $Y^*(k)$ is, from a mathematical point of view, an estimate of the total variation of Y over day k). An interesting and timely question is the predictability of the $Y^*(k)$ series, as part of the important problem of space weather forecasting. In the present paper, we will simply compute the auto-correlation function of $Y^*(k)$ for the six years long series of Chambon la Forêt (2190 data points). Figure 12 represents the auto-correlation $C_{Y^*}(\theta)$ of $Y^*(k)$. The 27-day periodicity of the activity function clearly appears in $C_{Y^*}(\theta)$. The second interesting feature is the value of the auto-correlation for a 1-day lag: $C_{Y^*}(1) = 0.61$, which indicates predictability. Nevertheless, the auto-correlation drops fast: only 0.35 for a two-day lag, which tends to indicate that long-term prediction is not possible. In a next work, we will apply methods used in seismology, like the (η, τ) Molchan [1997] diagram to the forecasting of magnetic activity, using again $Y^*(k)$. More precisely, we will assess rigorously the statistical significance of the forecasting. Let us recall that $Y^*(k)$, as demonstrated above, is a representation of $R^*(k)$ and is of worldwide significance.

The same analysis we performed here with 24 hours daily averages of one-minute value absolute first differences can be performed with hourly averages. Prediction studies will be richer.

Finally, an interesting topic is the influence of the conducting Earth on the values $|F'(t)|_T$. Taking first absolute values and then averaging makes the induction contribution more difficult to separate. In counterpart, it can be estimated with a high accuracy.

References

- Achache, J., J.-L. Le Mouél, and V. Courtillot, Long-period geomagnetic variations and mantle conductivity: an inversion using Bailey's method, *Geophys. J. R. Astron. Soc.*, 65, 579–601, 1981.
- Banks, R. J., Geomagnetic variations and the electrical conductivity of the upper mantle, *Geophys. J. R. Astron. Soc.*, 17, 457–487, 1969.
- Bellanger, E., E. M. Blanter, J.-L. Le Mouél, M. Mandea, and M. G. Shnirman, On the geometry of the external geomagnetic irregular variations, *J. Geophys. Res.*, 2001.
- Blanter, E. M., M. G. Shnirman, and J.-L. Le Mouél, Solar activity and variability of geophysical time se-

- ries; the synchronizing driving force, *J. Geophys. Res.*, submitted.
- Fukushima, N., and Y. Kamide, Partial ring current models for worldwide geomagnetic disturbances, *Rev. Geophys. Space Phys.*, *11*, 795–853, 1973.
- Hulot, G., A. Khokhlov, and J.-L. Le Mouél, Uniqueness of mainly dipolar magnetic fields recovered from directional data, *Geophys. J. Int.*, *129*, 347–354, 1997.
- Jankowski, J., and C. Sucksdorff, *Guide for Magnetic Measurements and Observatory Practice*, IAGA, 1996.
- Khokhlov, A., G. Hulot, and J.-L. Le Mouél, On the Backus effect—I, *Geophys. J. Int.*, *130*, 701–703, 1997.
- Mayaud, P. N., Morphology of the transient irregular variations of the terrestrial magnetic field, and their main statistical laws, *Ann. Géophys.*, *34*, 243, 1978.
- Molchan, G. M., Earthquake prediction as a decision-making problem, *Pure Appl. Geophys.*, *149*, 233–247, 1997.
- Olsen, N., Long-period (30 days–1year) electromagnetic sounding and the electrical conductivity of the lower mantle beneath Europe, *Geophys. J. Int.*, *138*, 179–187, 1999.
- Trigg, D. F., and R. L. Coles, *Intermagnet Technical Reference Manual*, 1999.

E. Bellanger, Fatma Anad, J.-L. Le Mouél and M. Manda, Laboratoire de géomagnétisme, Institut de Physique du Globe de Paris, 4, place Jussieu, 75252 Paris Cedex 05, France. (e-mail: ebellan@ipgp.jussieu.fr; anad@ipgp.jussieu.fr; lemouel@ipgp.jussieu.fr; mioara@ipgp.jussieu.fr)

Received October 5, 2001

This preprint was prepared with AGU's L^AT_EX macros v5.01, with the extension package 'AGU++' by P. W. Daly, version 1.6b from 1999/08/19.

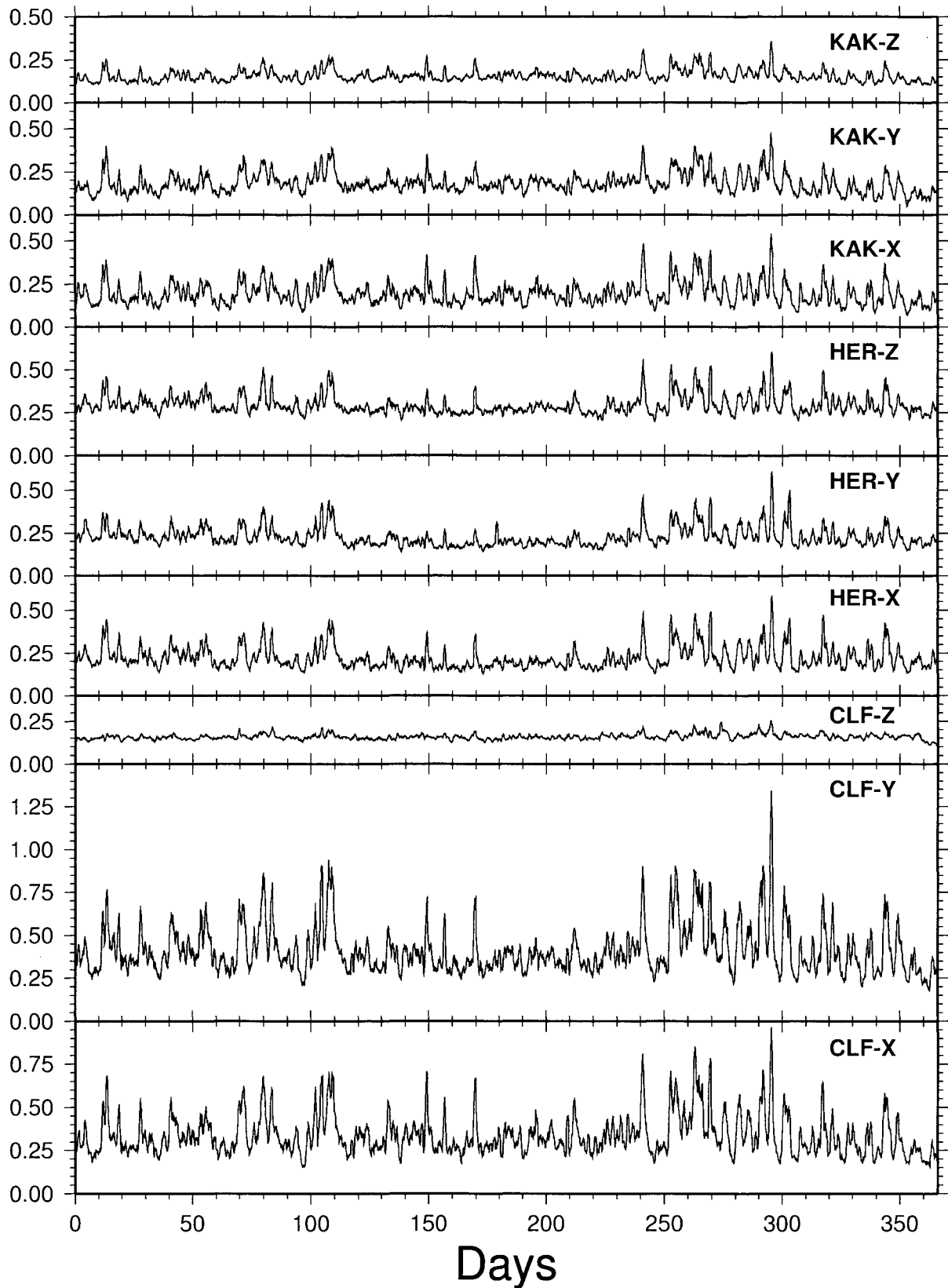


Figure 1. Averaged absolute derivative of the three components of the magnetic field in CLF, HER and KAK observatories for year 1996 (units are nT/min).

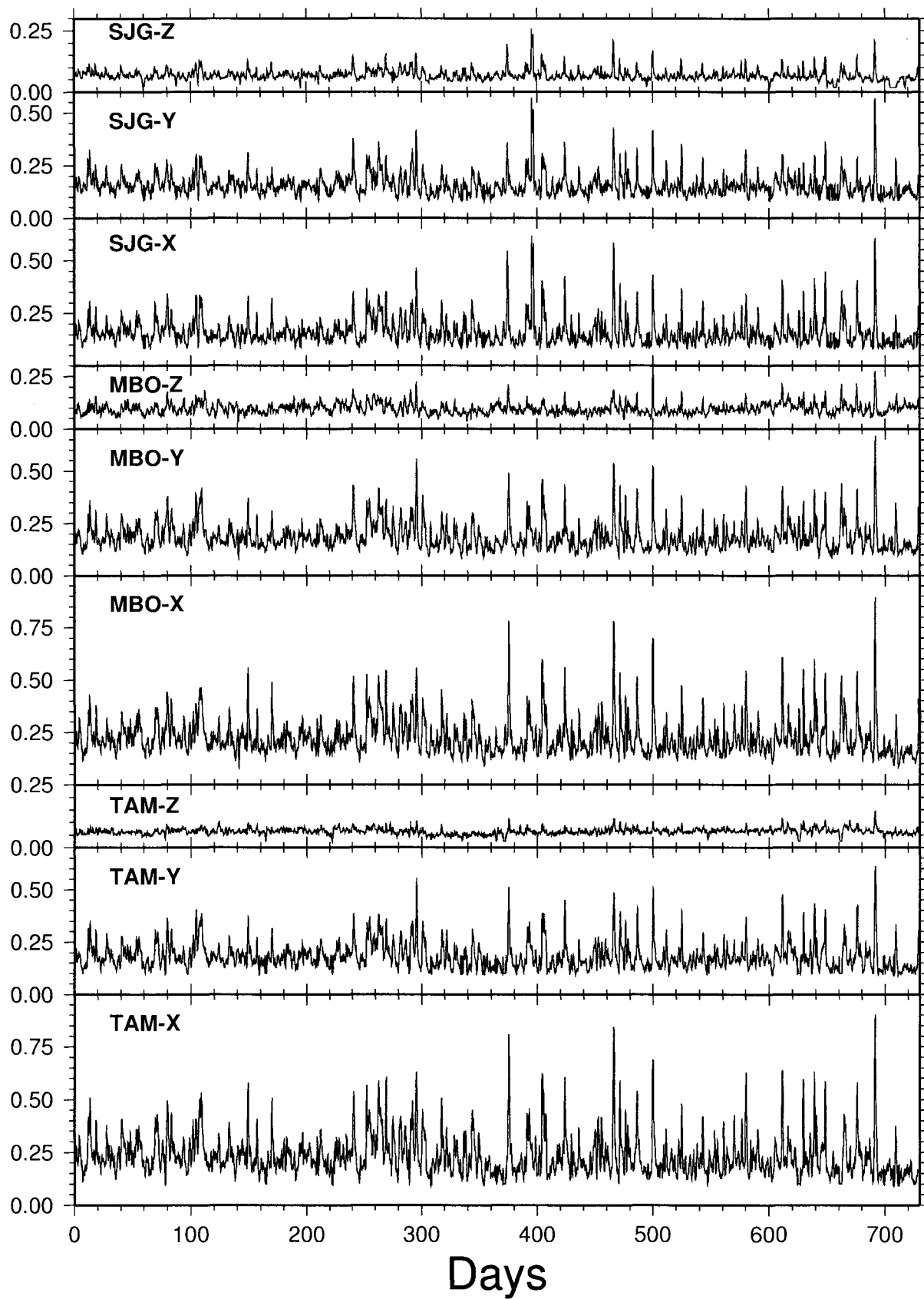


Figure 2. Averaged absolute derivative in TAM, MBO and SJG observatories for years 1996 and 1997 (units are nT/min).

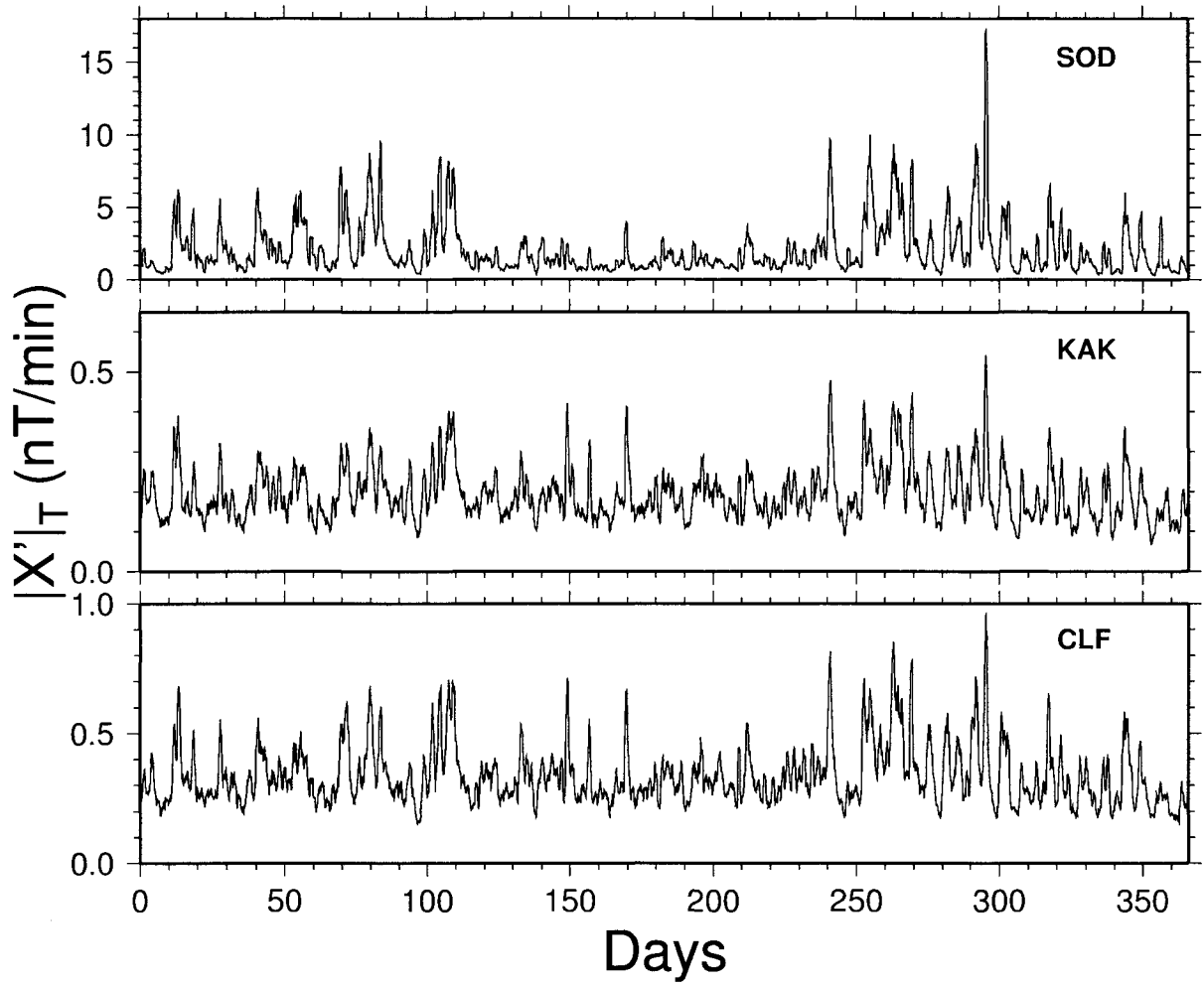


Figure 3. $|X'|_T$ in CLF, KAK and SOD for year 1996.

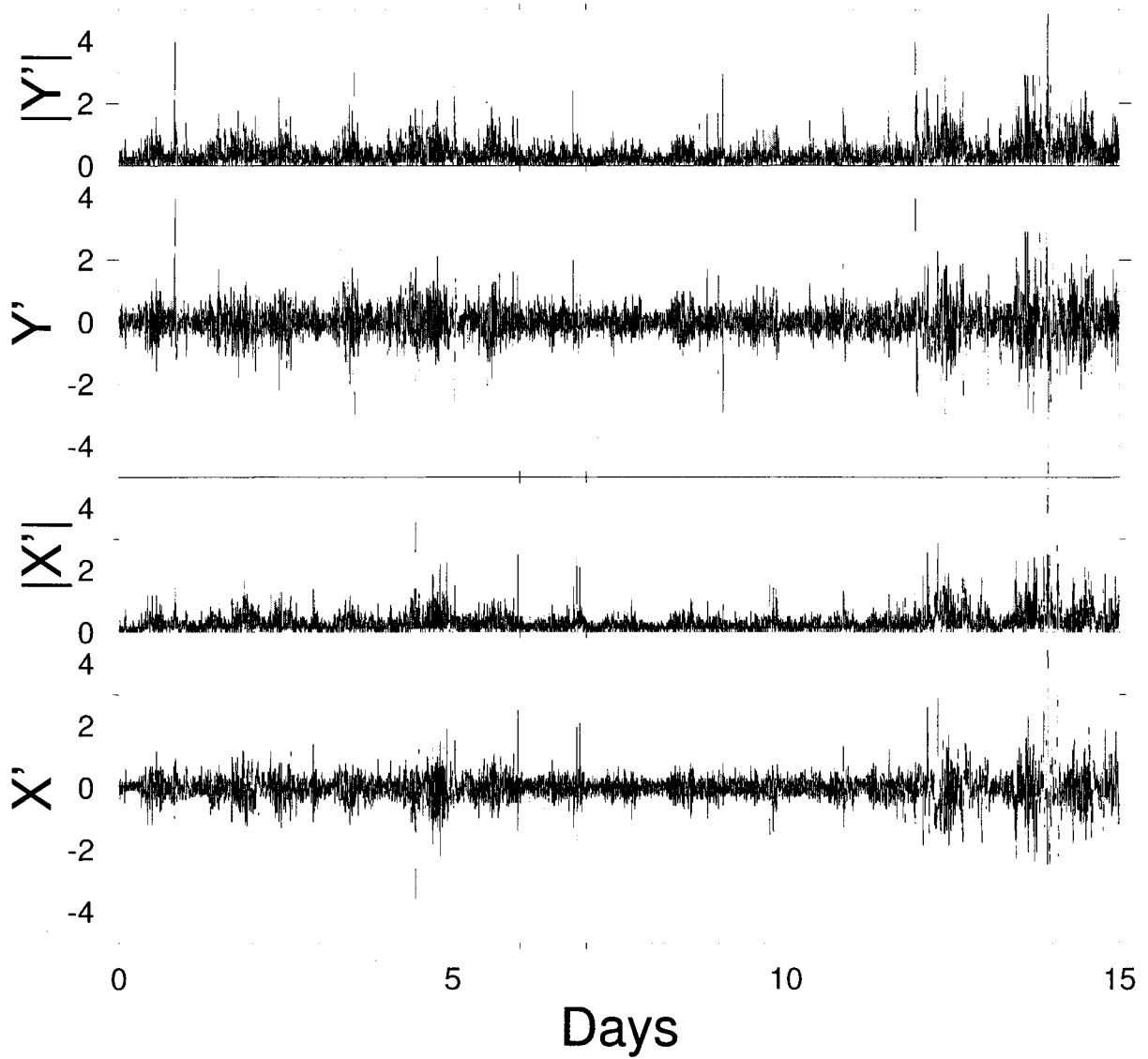


Figure 4. From bottom to top, X' , $|X'|$, Y' , $|Y'|$ in CLF for the first fortnight of 1996.

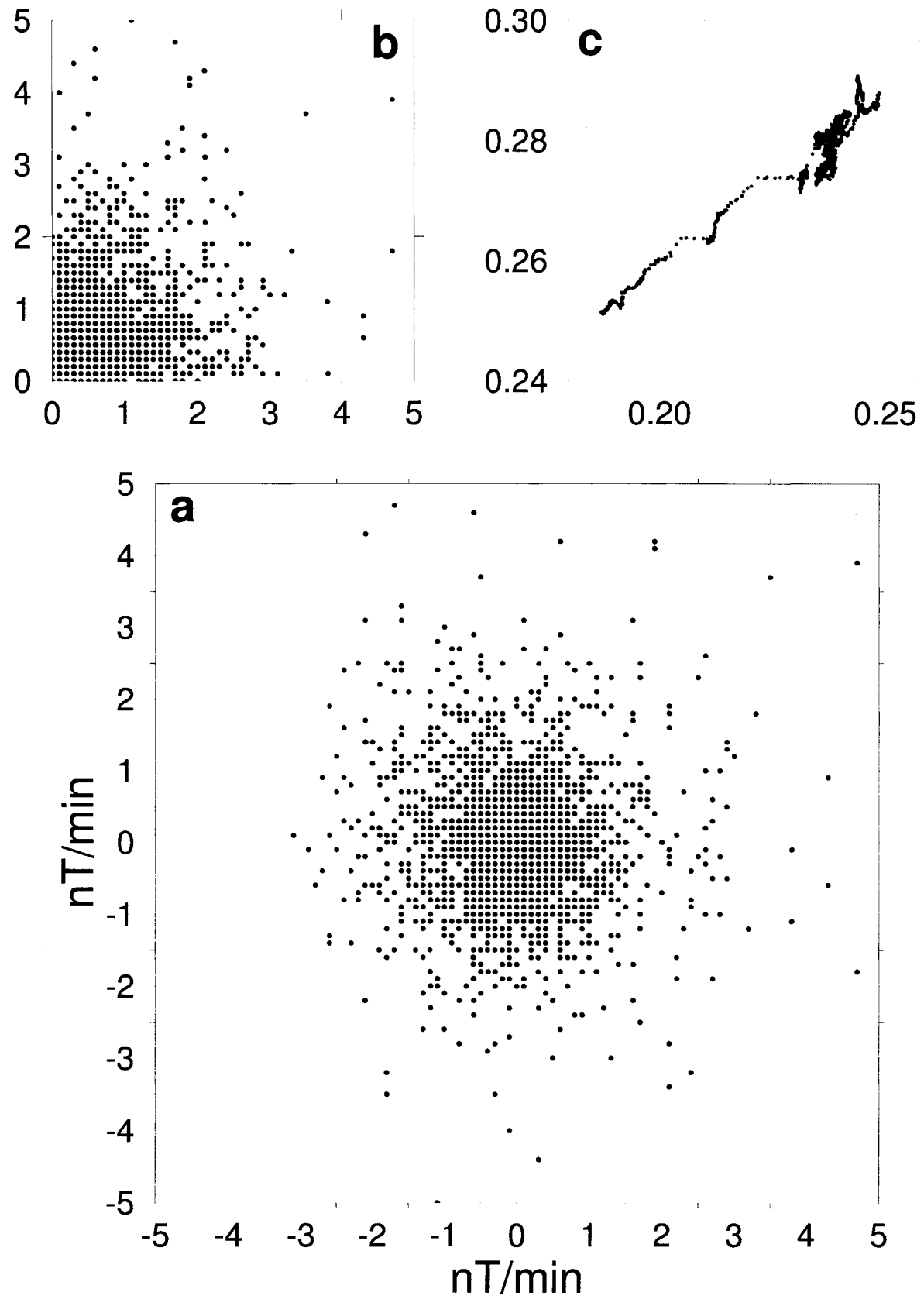


Figure 5. Phase diagrams in CLF for January 13th and 14th, 1996 (perturbed days). a) Y' vs X' ; b) $|Y'|$ vs $|X'|$ and c) $|Y'|_T$ vs $|X'|_T$ (units are nT/min).

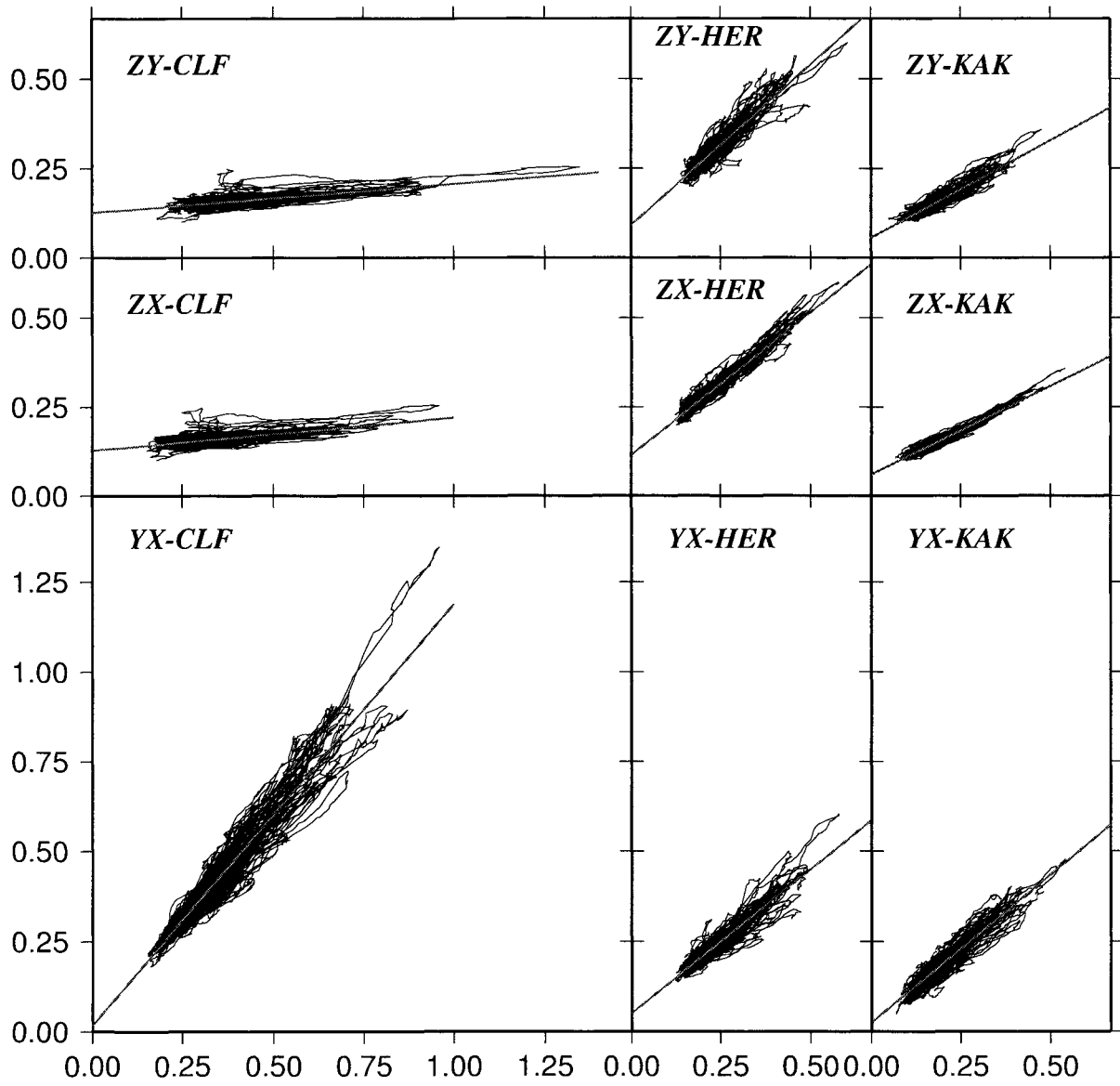


Figure 6. Polarisation diagrams in CLF, HER and KAK observatories for years 1996 and 1997.

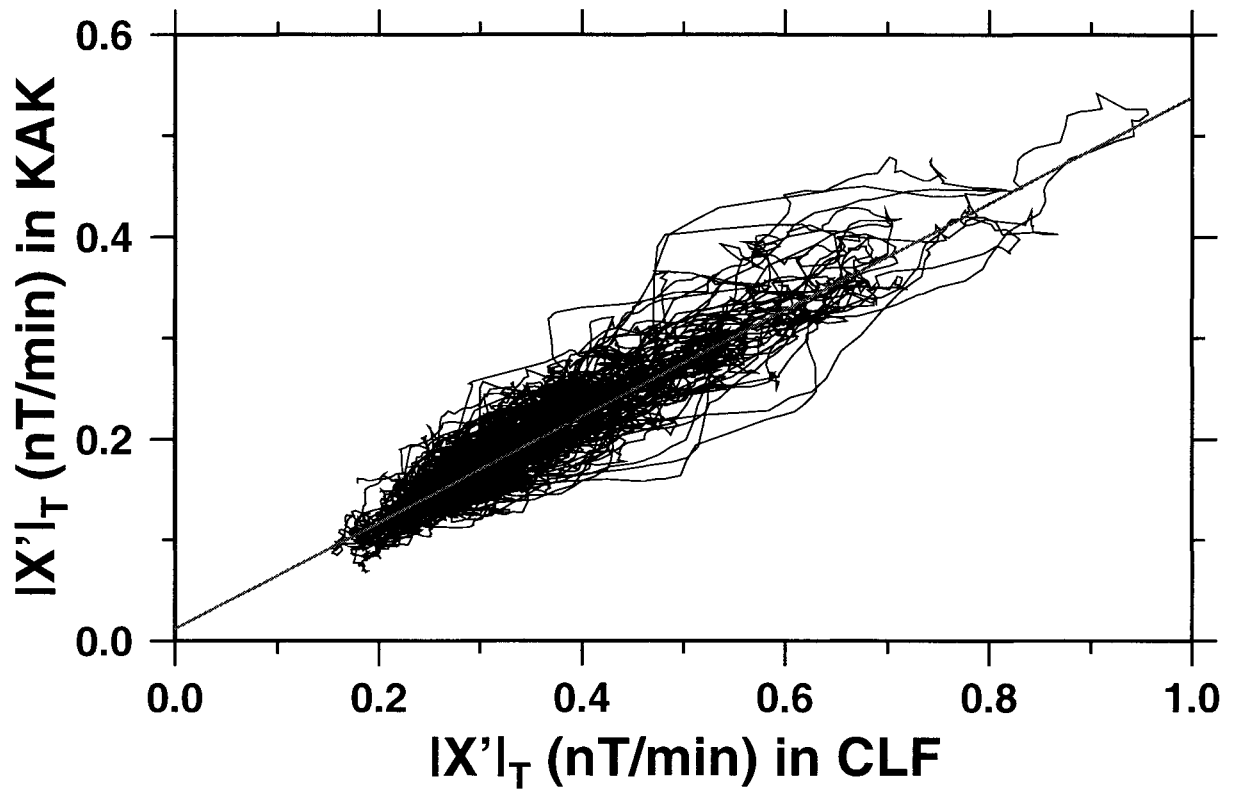


Figure 7. Polarisation diagram $|X'|_T$ in CLF *vs* $|X'|_T$ in KAK for years 1996 and 1997. The correlation coefficient is 0.93.

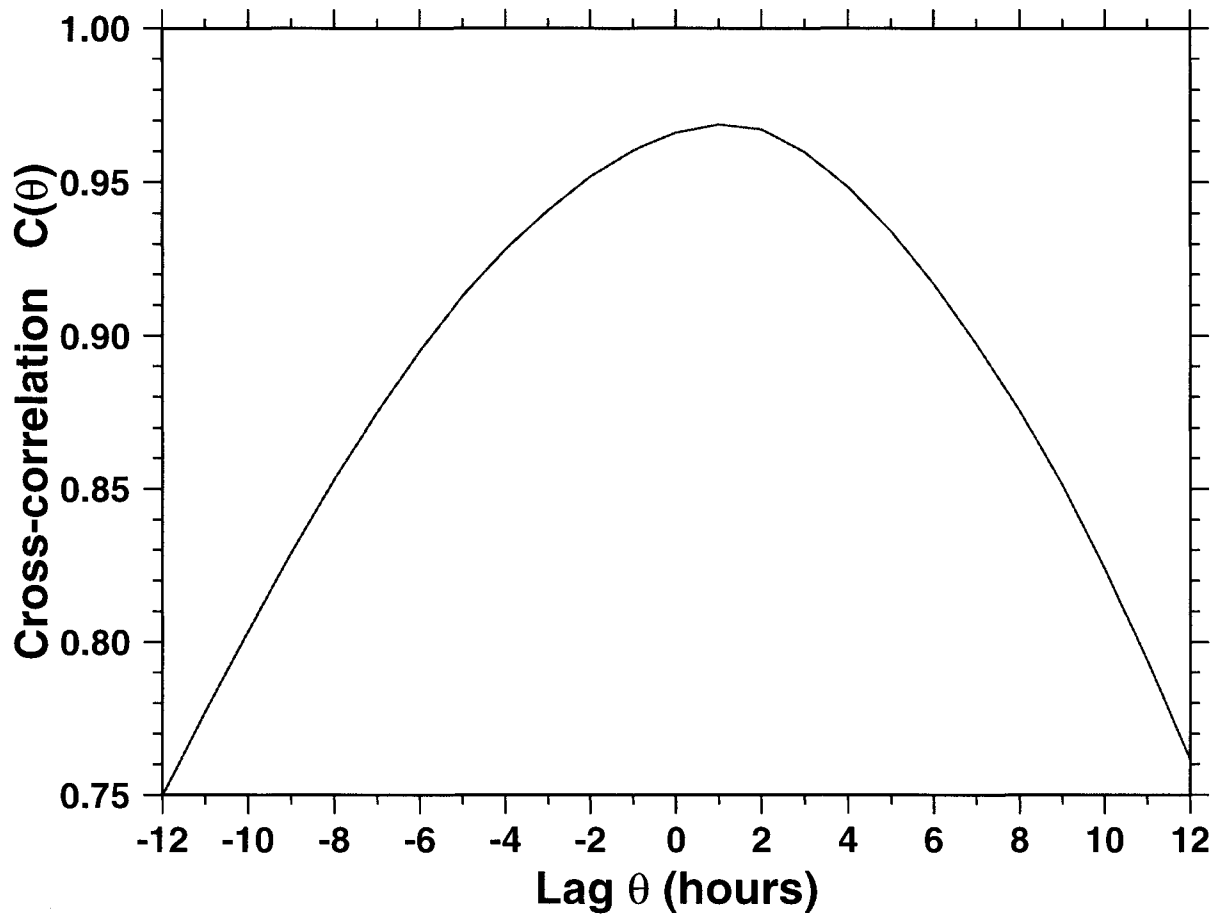


Figure 8. Correlation coefficient $c(\theta)$ between $|X'(t)|_T$ in Chambon la Forêt and $|X'(t + \theta)|_T$ in Kakioka, in function of θ for a period of 15 perturbed days.

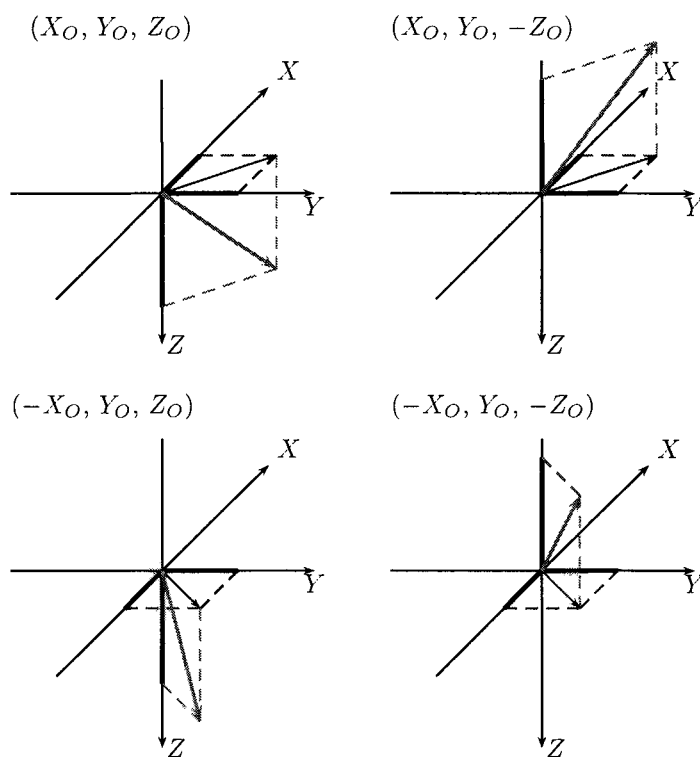


Figure 9. Different possible directions for $\omega(O)$ at an observatory O ; (X_O, Y_O, Z_O) corresponding to D_O, I_O ; $(X_O, Y_O, -Z_O)$ to $D_O, -I_O$; $(-X_O, Y_O, Z_O)$ to $(\pi - D_O), I_O$ and $(-X_O, Y_O, -Z_O)$ to $(\pi - D_O), -I_O$. Four other possible orientations can be obtained by changing Y_O to $-Y_O$.

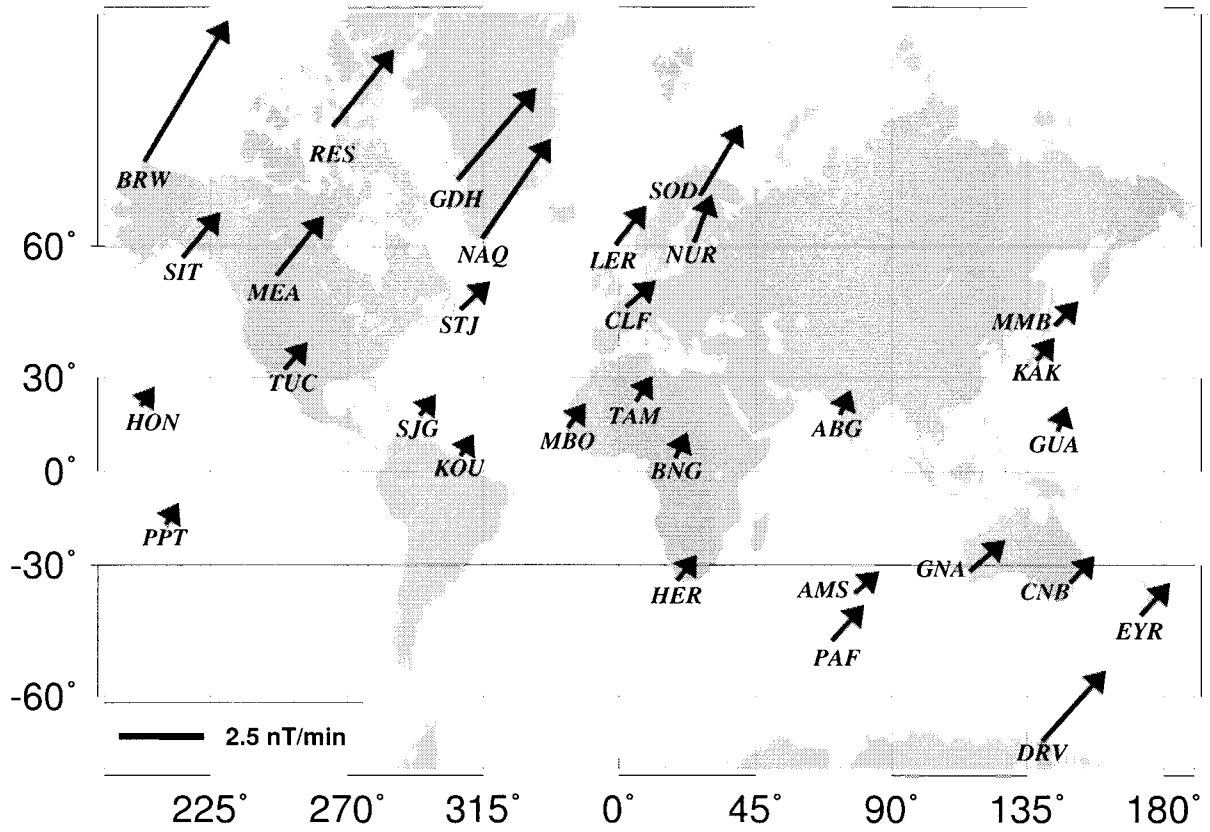


Figure 10. Map of a chosen direction and the length of the horizontal component ω_{\perp} of ω (we have taken X and Y , the components of ω_{\perp} , positive in every observatory, but symmetric orientations with respect to Ox or Oy axes are possible from the analysis at an individual station; see text). IAGA observatory codes are used.

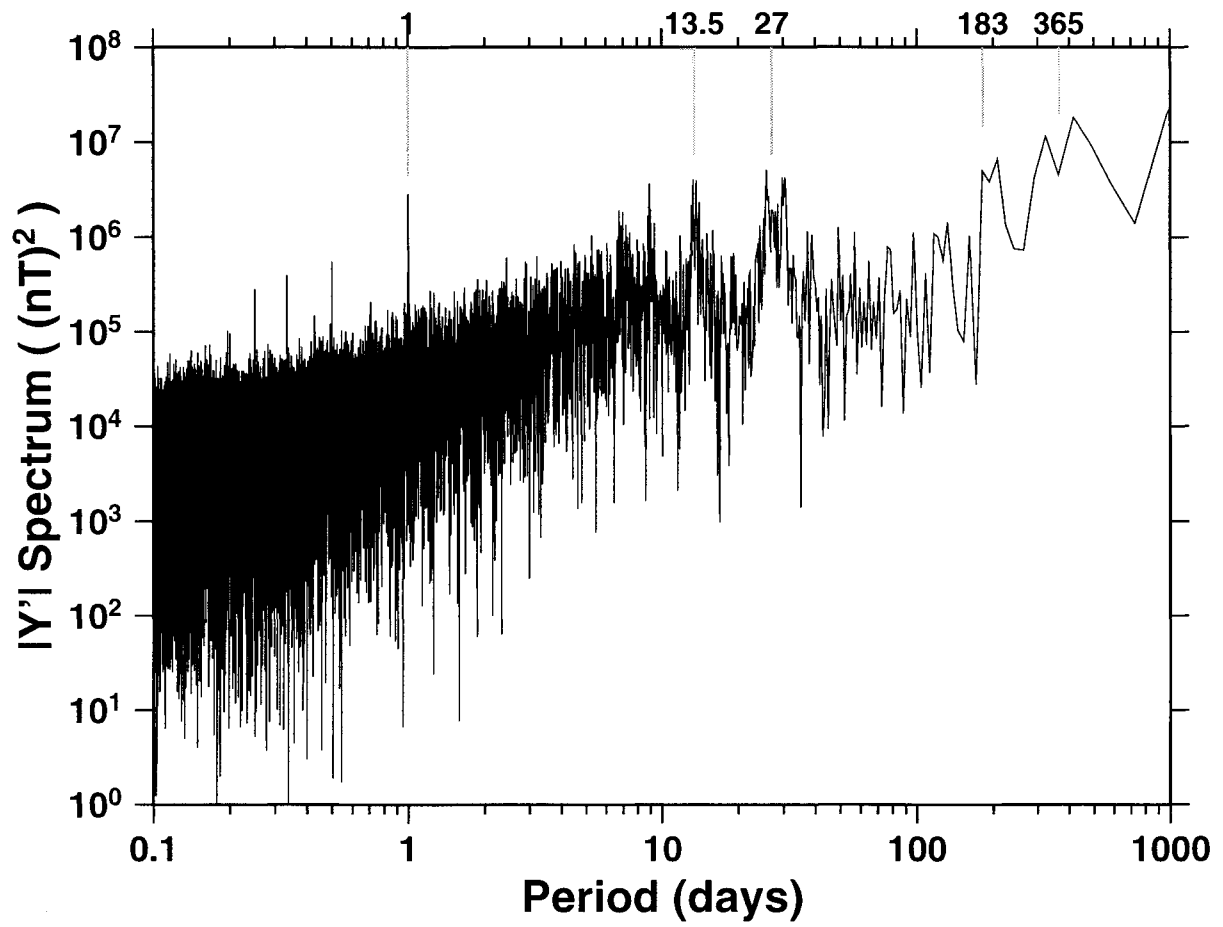


Figure 11. Energy spectrum for 6 years of absolute minute differences of the East component of the magnetic field ($|Y'|$) in CLF.

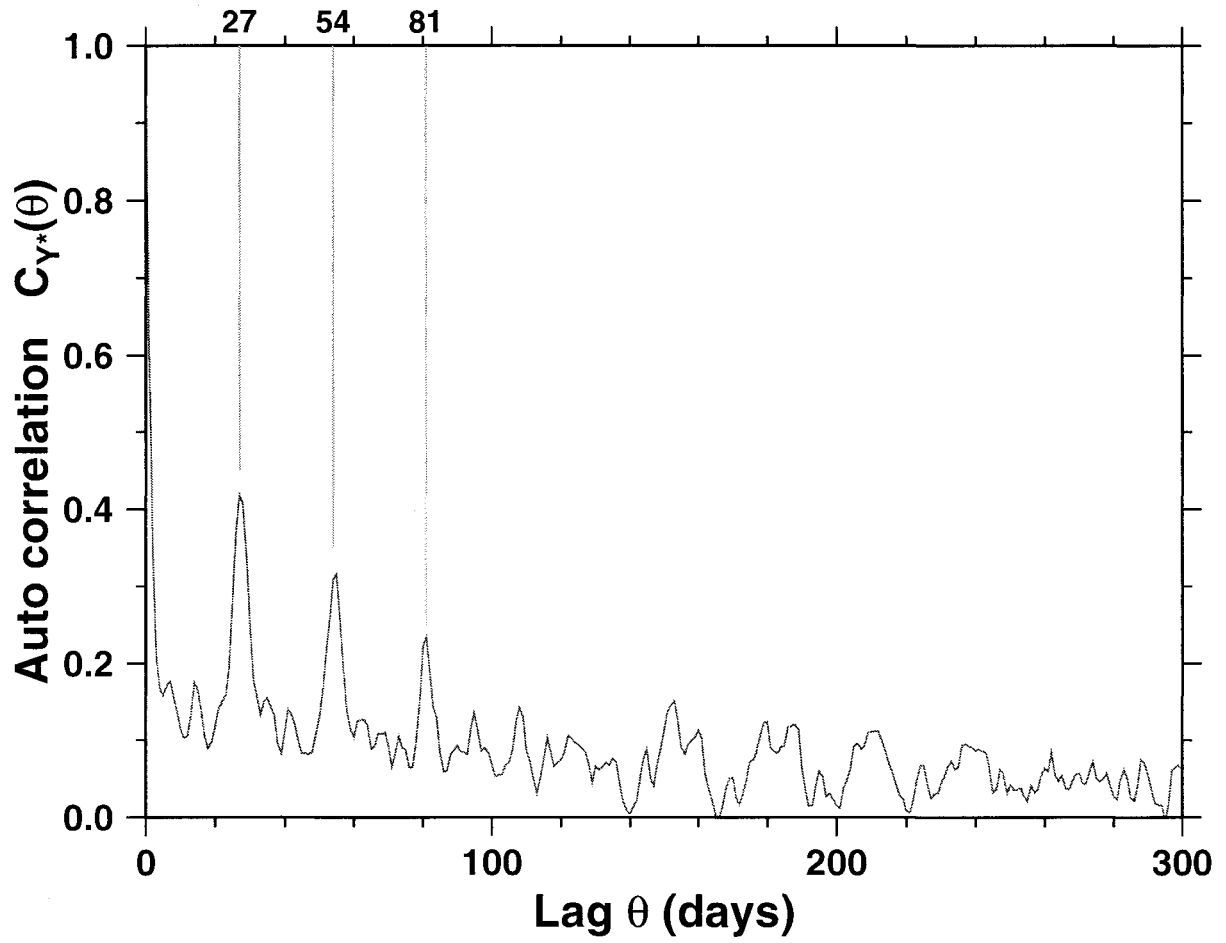


Figure 12. Auto-correlation $C_{Y^*}(\theta)$ of $Y^*(k)$ (see text) in CLF (six years of data).

On the geometry of the geomagnetic irregular variations

E. Bellanger, E. M. Blanter¹, J.-L. Le Mouél, M. Manda, M. G. Shnirman¹

Institut de Physique du Globe de Paris, France.

Short title: ON THE GEOMETRY OF THE GEOMAGNETIC IRREGULAR
VARIATIONS

¹Permanent address: International Institute for Earthquake Prediction Theory and
Mathematical Geophysics, Moscow, Russia.

Abstract. Using a simple non-linear signal analysis tool, we are able to picture some characteristics of the geomagnetic irregular variations. No distinction between disturbed and quiet days is made. The so-obtained irregular variations field is found to have quite simple time and space properties.

1. Introduction

The geomagnetic field is the sum of an ingredient of deep internal origin, the so-called main field, generated by the geodynamo working in the fluid core, an ingredient of superficial internal origin, generated by the magnetized rocks of the crust, and an ingredient of external origin, generated by electric currents flowing in the ionized layers of the atmosphere and further in the magnetosphere. The main field, which varies smoothly in time, is measured from time to time by magnetic satellites, and its temporal variations have been monitored, up to now, by magnetic observatories. The external field geometry and time constants appear quite complicated. It covers a large frequency spectrum, from a few kHz to the 22 years solar cycle. A lot of efforts have been devoted to characterize this external field, notably, in reason of its complexity and the huge amount of data required for its measurement (joined to the lack of computers in the former times), *via* the construction of magnetic indices [e.g. *Fukushima and Bartels*, 1956; *Sugiura*, 1964; *Davis and Sugiura*, 1966; *Allen*, 1972; *Rostoker*, 1972; *Svalgaard*, 1976; *Rangarajan*, 1989]. We won't resume here the long story of these indices, referring to *Mayaud* [1980] monograph, "Derivation, meaning and use of geomagnetic indices".

We just insist, quoting Mayaud, on two qualities required from an index to be useful: "any geomagnetic index should correspond to a single and well defined phenomenon and should be derived in such a manner that the data used be consistent with this phenomenon". To be simple, let us just recall that transient variations of the external field can be classified in regular and irregular variations: the former are

due to permanent sources of field which cause the regular occurrence, every day, of a certain variation during certain local time hours at a given point of the Earth; the latter correspond “to sources which do not permanently exist, and, hence, their occurrences is basically irregular”. So, magnetic indices are devoted to characterize either the regular variations or the irregular ones — or rather in the latter case, some component of the irregular variations.

In fact, the present paper has not the objective to derive a new index. It is at the same time more and less ambitious. More, because we will consider a vector field, with a geometry, and not a simple scalar like K_p , am , aa , Dst (which have a global meaning, although derived from measurements in an array of observatories). Less, because we will limit our sampling to one value per day and take long running averages; so, short time constants cannot be addressed in the present study (but they will be in a following one).

In fact, we will use very simple tools, essentially an average non-linear (or absolute) derivative [*Blanter et al.*, submitted; *Bellanger et al.*, submitted]. The method, however simple, is quite powerful to reveal hidden structure in complicated time-series.

2. The data

The present study has been performed on observatory hourly means obtained from the World Data Center (WDC - Copenhagen, Denmark), or directly from the observatories. The first criterion in observatory selection was the length and continuity of the available time-series of the horizontal northward (X) and eastward (Y) components (directly available or computable from declination (D) and horizontal intensity (H)),

and of the vertical downward component (Z).

Hourly mean values centered on the half hour have been computed from one-minute values recorded digitally since flux-gate systems have been introduced in the observatories (the date of this introduction varies from an observatory to another). Prior to this, hourly mean values were scaled by hand from photographically recorded magnetograms. In early years of operation, problems were encountered in measuring the vertical component (Z), the noise level being higher (a further point worth noting is that in the early years the hourly mean values were centered on the hour; when these values were digitized, means between two adjacent hours were computed to center the means on the half hour).

Following this initial selection, all time-series have been subjected to a careful validation. We checked the consistency of the hourly mean series with the monthly mean series [*Alexandrescu, 1998*]; this revealed that in some observatories and at certain epochs changes in the baseline levels had to be applied to the hourly means. We corrected for this by simply applying the required changes to the hourly series; in the case this correction did not give satisfying results, more information was directly requested from the observatories.

Finally, 21 series are retained in our analysis, chosen in reason of their length and quality. We had to accept some gaps in some of them; a linear interpolation was used to reconstruct the missing values. In case of a long gap, the time-series was split into two sub series (GUA, HON, TUC, *c.f.* table 1). The list of available observatories with the corresponding code, geographical coordinates and lengths of time-series is given

in table 1 (note that further data will be obtained from other observatories). Let us emphasize that the process of establishing the time-series in the way just described, however time consuming, is both an essential step of the following analysis and a very efficient way of identifying possible defects in the observatory data.

We will also present series relative to the *aa* index. Let us recall what this index is. It is aimed at characterizing the planetary level of the irregular variations as a whole, without any discrimination between its different species [Mayaud, 1980]. At a given observatory, the *K* index measures the range of the magnetic variations (the regular part of these variations, S_R according to Mayaud's notation, being removed) on horizontal components, over consecutive three hours intervals [Bartels *et al.*, 1939; Mayaud, 1967]; the value of the index is a semi-logarithmic function of the range. The planetary K_p index is computed by averaging the *K* index from a dozen of magnetic observatories. Mayaud proposed an improved planetary index, *am*, based on magnetograms from 27 better-distributed observatories, the activity in a 3-hours interval being expressed, like the ranges, in nT [Mayaud, 1980]. As data from 27 observatories has not been available for a long time, in order to get a longer series, Mayaud [1972] built the series of *aa* index from the data of only two antipodal magnetic observatories; this series has been regularly implemented since 1973 by M. Menvielle [Menvielle and Berthelier, 1991].

3. The non-linear derivative

We have $3 \times M$ series $X_m(t_n)$, $Y_m(t_n)$, $Z_m(t_n)$, $m = 1, 2 \dots M$; M is the number of observatories, t_n is time, reckoned in days; the range of n is different for each

observatory. Let $F(t)$ be one of these time-series and consider the non-linear derivative,

$$|F'(t)| = |F(t+1) - F(t)|, \quad (1)$$

and the average of $|F'(t)|$ on a sliding time window of length T ,

$$|F'(t)|_T = \frac{1}{T} \sum_{\tau=0}^{T-1} |F'(t+\tau)|. \quad (2)$$

$|F'(t)|_T$ is defined at $(N - T)$ points (N is the length of the time-series). In the present study, T is taken equal to 1 year, *i.e.* $T = 365$.

4. Results

The results are illustrated by figure 1; the graphs are referenced, for each observatory, by the relevant component $|X'|_T$, $|Y'|_T$, $|Z'|_T$ (that we will denote in a simpler way X , Y , Z in the following).

Two other series have been added for comparison, derived from the aa index. We consider the daily means of aa (for a given day, the average of the 8 aa values of this day), and compute the running annual mean of these daily values. This we call the $A_T(t)$ series:

$$A_T(t) = \frac{1}{T} \sum_{\tau=0}^{T-1} \overline{aa}(t+\tau), \quad (3)$$

where \overline{aa} is the daily mean of aa ; time in days, $T = 365$. We also compute the average non-linear derivative $|A'(t)|_T$ by (2). Series A_T and $|A'(t)|_T$ are displayed on figure 2.

Let us comment figures 1 and 2. First it is remarkable how all the X , Y , Z curves look alike. 1) In a given observatory, X , Y , Z look alike (although with small differences,

especially when the variations are small, which is to be expected). 2) The curves also look strikingly alike from an observatory to the other (see for example the X curves at Chambon la Forêt and Hermanus). And the A_T curve, and still more the $|A'(t)|_T$ curve look alike the X , Y , Z curves of the observatories.

The aa index is aimed to monitor, as said before, the irregular variations. For this purpose, when measuring the 3-hourly range, the S_R regular variation is removed by different techniques. Here we start from the daily averages of the magnetic components. Taking such an average also removes most of the regular variation; the S_R field indeed contains only a small zonal part. This question of contamination by S_R was addressed by Mayaud, when discussing the u index of geomagnetic activity, derived from an early work of *Moos* [1910] at Colaba in India. *Moos* defined the interdiurnal variability U of the horizontal component at a given station as the difference between the mean values for that day and for the preceding day taken without regard of sign (as our non-linear derivative). The u index is a combination of U indices from a few observatories [*Bartels*, 1932; *Chapman and Bartels*, 1940]. Mayaud observed that this u index can be contaminated by the regular variation S_R since its day-to-day variability should contribute to the interdiurnal variability U , and made a test to estimate this contamination; *Mayaud* [1980] was “astonished by its smallness”. It is legitimate to transfer this conclusion to the case of our daily absolute derivative. So we will consider that our series are relative to the irregular variations of the external field. The tight resemblance between the $|A'|_T$ derived from 3-hourly ranges and the X , Y , Z series derived from first differences of daily means is not trivial for all that.

dit?

A big advantage of the non-linear derivative is that it does not rely on the absolute values of the magnetic components. It is well known that the main difficulty in maintaining a high standard magnetic observatory is to obtain good absolute measurements, *i.e.* good baselines [e.g. *Jankowski and Sucksdorff*, 1996]. And the baselines of most observatories were of rather poor quality, except for the declination, before the introduction of proton magnetometers in the fifties (to say the truth, they still are in some places). But even with a poor absolute control, daily mean differences can be quite accurate and generally are (of the order of 1 nT). The contamination of the X , Y , Z by the S_R , however small, is certainly larger than the instrumental error. In fact, the level of the curves, or the line labelled zero on figure 1, is uncertain by a certain quantity, not necessarily constant on the whole considered time span. We will discuss this point while studying the field geometry.

5. The field geometry

Let us call $\Omega(P, t)$ the irregular variations field whose components at different observatories are X , Y and Z represented by figure 1; in practice the time sampling is one day and the current point P runs through the observatories P_m , ($m = 1, 2 \dots M$; M is 21 at the present time).

We start from the observation (approximate; we are dealing with data) that the components X , Y , Z relative to a given observatory are similar; the computation of the hodograph (figure 4 for CLF and HER), is particularly convincing, and shows a polarization independent of time (in a first approximation; we will come back to possible

small changes later). Even more, all the series, relative to different observatories, are similar. This implies that the time and space variations of $\Omega(P, t)$ separate:

$$\Omega(P, t) = \omega(P)R(t) , \quad (4)$$

$R(t)$, that can be taken positive, is an activity function, $\omega(P)$ characterizes the geometry of the irregular variations. A consequence of (4) is that we can analyze separately the geometry $\omega(P)$ and the time function $R(t)$. We will now present the first step of this analysis, postponing a more complete one till we have gathered as many series as possible.

The goal is to compute, at each point P , the direction of ω without introducing a bias due to the “noise” (in fact the sum of the instrumental noise and the S_R residual effect). For this, we compute the declination D (and in a similar way the inclination I) by a linear extrapolation of the graphs $Y(X)$ (figure 4); the slope of the regression line, $(Y/X)_{\text{ex}}$, is free of any bias due to the noise, while the intercept is linked to the noise level. The declination is then,

$$D = \tan^{-1} ((Y/X)_{\text{ex}}) . \quad (5)$$

Six examples of regression computation (three components of CLF and HER) are represented on figure 4, showing that the intercept is not zero. The error on the estimation of the slope is small enough for the precision being better than three degrees on D and I . We will later represent the horizontal component ω_{\perp} ; its norm cannot be computed from only the above ratios; indeed we compute $\|\omega_{\perp}\| = \sqrt{X^2 + Y^2}$, introducing a bias in the norm of ω_{\perp} .

Now, it is to be noted that all the quantities X , Y , Z are by definition positive. The cartesian components of ω are defined only within the multiplicative factor ± 1 . Four possible values result for D , and two for I (figure 3). In fact, the number of combinations is reduced from 8 to 4, since there is no need to distinguish between ω and $-\omega$ (ω is a transient field).

In this paper we will use simple regularity conditions to discriminate between the 4 possible solutions at each observatory. First, X clearly has the same sign everywhere, we will chose it positive. Let us first concentrate on the horizontal components of ω ; Y is given the sign which makes the vector distribution the most regular (figure 5; in fact, we resort to the second step of the analysis, to be described now, to help in the discrimination). Satisfactorily, irregular variations vectors from close observatories point closely in the same direction with a comparable horizontal component. The second step of the study is to find the best dipolar geometry matching the variations field ω (see section 6). It leads us to change from geographical coordinates to spherical coordinates with an axis \mathbf{d} different from the rotation axis (trying a wide range of latitudes and longitudes for this axis) until the variations field is aligned, with the best accuracy, along the magnetic meridians in the new coordinates system (bottom of figure 5). At the same time we checked that our choice of signs for X and Y was the best, according to this criterium. The same regularity condition was used to choose the sign of the vertical component.

The accuracy in the determination of θ_0 , the colatitude of \mathbf{d} , is very good (of about 3 degrees); the accuracy on ϕ_0 , its longitude is more imprecise (about 10 degrees; this

lesser accuracy is of course due to the weak value of the dipole latitude). The values found were $\theta_0 \simeq 14$ degrees and $\phi_0 \simeq -82$ degrees.

6. Discussion and conclusion

It appears that the $\Omega(P, t)$ variation field constructed in the very simple way described above exhibits a remarkably simple organization. As we showed, time and space variables separate (note that the graphs $|F(t + 1) - F(t)|$, without averaging, of course present some family likeness).

The time variation, expressed by the single scalar function $R(t)$ is of course linked with the solar activity time variation, as the *aa* index is [Ulich, 2000]; this function $R(t)$, and its relation with the solar activity will be studied in a next paper, using for example methods developed in *Blanter et al.* [submitted].

The geometry ω , quite simple, essentially presents the symmetry of an ~~external dipole~~, the colatitude and longitude of which are found to be 14 and -82 degrees (in fact, the parameters of \mathbf{d} cannot be said different from the parameters of the Gauss dipole of the internal main field). Let us recall that *Slaucitajs and McNish* [1937] (see also *Chapman and Bartels* [1940] p. 295) showed, as soon as 1937, that the horizontal vectors representing the difference between the daily means of (X) and (Y) (international disturbed minus international quiet days for 1927) tended to be aligned with the magnetic meridian.

Let us stress that departures from the dipolar symmetry are genuine in some places (not within the uncertainty on the computed directions). For example, the horizontal

component of ω is far from the meridian of the ($14^\circ, -82^\circ$) dipole at the station of AIA, whose location is unusual, at the end of a narrow peninsula (figure 5); significant (however small) departures are also found in high latitude observatories.

At this stage, we have not performed any complete spherical harmonic analysis, postponing it to when we have collected the maximum number of series. Note that the $\Omega(P, t)$ field contains an internal part, due to induction in the conducting solid Earth, and ocean. It will be possible to make the analysis directly with the absolute values X , Y , Z , using the methods developed in *Hulot et al.* [1997]; *Khokhlov et al.* [1997].

As said earlier, we have only eliminated the regular variation, or S_R (or rather most of it), addressing the irregular variation field as a whole, without discrimination between its different species (ring current, auroral variations, DP2 variations, *etc* [*Mayaud*, 1978]). Our main result is that a very simple organization can be derived from a rather intricate data set.

References

- Alexandrescu, M., Database of geomagnetic observatory monthly means seeks contributors, *Eos AGU*, 79, 345, 1998.
- Allen, J. H., Auroral electrojet magnetic activity indices (*AE*) for 1970, *Report UAG 22*, World Data Centre A for STP, NOAA, Boulder, Colorado, 1972.
- Bartels, J., Terrestrial-magnetic activity and its relation to solar phenomena, *Terr. Magn. Atmos. Elec.*, 37, 1, 1932.
- Bartels, J., N. H. Heck, and H. F. Johnston, Geomagnetic three-hour-range indices for the years 1938 and 1939, *Terr. Magn. Atmos. Elec.*, 44, 411, 1939.
- Bellanger, E., E. M. Blanter, J.-L. Le Mouël, and M. G. Shnirman, Estimation of the 13.63-day lunar-tide effect on length of day, *J. Geophys. Res.*, submitted.
- Blanter, E. M., M. G. Shnirman, and J.-L. Le Mouël, Solar activity and variability of geophysical time series; the synchronizing driving force, *J. Geophys. Res.*, submitted.
- Chapman, S., and J. Bartels, *Geomagnetism*, vol. 1, Oxford Univ. Press, 1940.
- Davis, T. N., and M. Sugiura, Auroral electrojet activity index *AE* and its Universal Time variations, *J. Geophys. Res.*, 71, 785, 1966.
- Fukushima, N., and J. Bartels, A *Q*-index for the geomagnetic activity in quarter-hourly intervals, *Abh. Akad. Wiss. Göttingen Math. Phys. Kl.*, 2, 1956.